

Robocasting Periodic Lattices For Advanced Filtration

John N. Stuecker, Joseph Cesarano III, James, E. Smay
Sandia National Laboratories
Albuquerque, NM 87185

Abstract

Ceramic filters used in the casting of molten metals are commonly created by slurry impregnation of polymeric foams, yielding a fired ceramic foam structure. These foam structures have high part-to-part standard deviation in flow rates (~25%) and have weak sections which can fragment into the melt. In contrast, periodic lattice filters (PLF's) made by robocasting have a cross-hatched face-centered-cubic arrangement of rods. As such, the robocast filters have high strength and may be easily tailored to offer a specific internal pore structure to control the flow rate and pressure drop across the filters. Standard deviation of flow rates among PLF's are less than 1%. This paper describes the methodology of creating PLF's as possible foam filter replacements.

Introduction:

The most commonly used ceramic filters on the market today are thin-walled extruded honeycomb and ceramic foam filters. Extruded honeycomb filters are employed in most automobile exhaust systems and are commonly used as catalyst supports. These filters are made by extruding a plastic ceramic body through a die which yields parallel walled channels. Very well defined pore sizes result from this fabrication method. Ceramic foam filters are made by immersing a polymeric foam into a ceramic slurry. The slurry-saturated foam is then drawn through a set of rollers which displace excess slurry, allowing the pore structure of the foam to become prominent. The polymeric foam is then burned out and the resulting ceramic structure fired to high density. Pore sizes are inherently variable and difficult to reproduce. Non-uniform pore structure leads to inconsistent flow rates for any particular filter. Flow rate control is important when performing metal casting. Further, regions of closed pores occur, as well as regions of very thin/weak ceramic struts. These ceramic foams are most commonly used in filtering oxides from molten metals, with the major issues being variability of porosity resulting in variable flow rates, and fragments of ceramic foam breaking off during filtering, flowing into the casting.

Robocasting of high solids loading slurries allows precise placement of material in three dimensions. By slightly flocculating the slurry, spanning structures can be built and are similar in appearance to stacks of rods with maximum span distances of up to eight times the rod diameter. The rod-like shape of the extruded material is directly created from the circular extrusion orifice. Moving the orifice back and forth in a controlled pattern while extruding the ceramic material allows precise layering of these rods in a periodic lattice and a unique style of ceramic filter to be created. The freshly-extruded slurry melds together with the previously placed rods thereby creating a strong lattice. These filters can have user specified pore size between the solid rods by altering the extrusion path (80 to 3000 μm) as well as having a range of rod sizes by altering the orifice size (80 to 3000 μm). Further, line-of-sight porosity in the flow direction can be eliminated in four build layers by using equal rod size and pore size, and placing the rods in a face-centered cubic (FCC) pattern. This style of filter may be used in applications currently using the extruded honeycomb and ceramic foam structures. This discussion will compare flow properties of ceramic foam and periodic lattice filters.

Experimental:

Alumina ceramic foam filters used commercially in molten metal filtration were generously provided by Selee Corp., Hendersonville, SC (Figure 1a). Standard foams are available in 20, 30, 45, and 60 pores per linear inch (ppi). The foams are present inside a solid, pressed alumina ring, yielding an overall part size of approximately 1" OD, and 0.4" thick through the porous foam.

Periodic lattice filters (PLF's) were fabricated by robocasting an aqueous based 60 vol%, 99.8% purity alumina slurry containing less than 0.5 vol% organic material. Yield stress of the slurry was increased until unsupported lattices could be fabricated. Filters of various pore sizes, rod diameters, and thicknesses were created in attempt to characterize air and liquid flow through the periodic lattices. All PLF's were dried for several hours and fired to 1650°C to near full density. A PLF with 30 ppi is shown in

Fig. 1b. PLF's were created that match first, the geometry of the commercially available foams, and then second, the liquid flow rates. Three of each filter geometry were fabricated and characterized to obtain standard deviations. Table 1 displays a selection of tip sizes used in the robocasting process, the resulting sintered rod diameter, the resulting linear ppi of the FCC lattice, and equivalent surface areas. The surface area data is provided simply for comparison to commercially available extruded honeycomb structures. For example, ultra-thin-walled honeycomb used as a catalyst support with 24.5 ppi yields a surface area of $\sim 98 \text{ in}^2/\text{in}^3$, which is very similar to a 25 ppi PLF ($99 \text{ in}^2/\text{in}^3$).

Air permeability tests were performed by inserting the PLF into a controllable air-flow chamber. Taps just before and after the test specimen allowed monitoring of pressure drop via a digital manometer accurate to $\pm .1$ psi. The air flow rate was adjusted from 1 to 7 cubic feet per minute (cfm) while pressure drop readings were taken. Using the resulting data and Darcy's equation, the permeability constant was calculated:

$$K_d = \frac{QL}{A\Delta P}$$

where Q is the volumetric flow rate, L is the length of the permeate, A is the cross-sectional area, and ΔP is pressure drop across the permeate. Liquid flow rate was measured using water at a constant head of water of 10 psi. The amount of time required to fill a gallon container was timed, and flow rates were recorded in gal/min. It is suitable to use water in the liquid flow tests to get a general idea of the flow rate of molten aluminum due to the very similar Reynolds numbers.

Results and Discussion:

In order to eliminate unimpeded line-of-sight flow channels in the flow direction, PLF's were fabricated with layers of stacked rods with the spacing between the rods equal to the rod diameter. A unit cell consists of four layers. Permeability data for several PLF's are found in Figure 2. The plot contains data for PLF's of 14 to 47 ppi, with one, two, and three unit cells in thickness. The trend in the plot is expected. Decreasing the rod diameter (thus increasing the ppi), restricts flow, increasing the permeability constant K_d . Increasing the number of layers of the PLF for a given pore size also increases K_d , further restricting flow. One notable feature arises from the graph, the permeability constant is not constant. Rather, a decrease in the permeability constant is seen with increasing flow rates. This change in K_d is most likely due to change in gas flow from laminar to turbulent. What parts of the graph are turbulent and what parts laminar? Regardless of laminar or turbulent flow, Fig. 2 may be used as a map to design a PLF with a specified flow rate by selecting the appropriate thickness and ppi values. For example, if a high surface area is needed for a catalyst support, smaller rod sizes yielding larger ppi values are required. However, it may then be necessary to select a small number of layers in order to achieve an acceptably high flow rate.

Often, pressure drop across a filter is an important parameter. Figure 3a-c compares the pressure drop across a 45 ppi foam, a 30 ppi foam, and a 47 ppi lattice. The 47 ppi lattice has the same physical geometry as the foam filters (1" OD, 0.4" thick). For the three samples of each filter, it can be seen that the foam structures have lower pressure drop than the PLF. The very low bulk density of the foam structures ($\sim 80\%$ porosity) accounts for the lower pressure drop. However, the foam filters show very high part-to-part standard deviations relative to the PLF. From the back-lit foam structure in Figure 1, it is inferred that the inconsistent pore structure inherent in the slurry impregnation process accounts for the standard deviation among samples. The back-lit PLF in Figure 1 conveys the good uniformity and consistency of the internal structure. In conclusion, for a specific ppi value, if it is desired to achieve a low foam-like pressure drop with a PLF then the PLF must be fabricated relatively thinner than the foam. This may or may not pose a problem related to reduced filtration efficiency. It is believed that PLF's may be effective filters even when relatively thin since the flow path is inherently tortuous and line-of-sight flow channels may be completely eliminated in a single unit cell. Conversely, thin foam samples run the risk of exposing straight-through flow channels. The filtration efficiency of PLF's will be an area of future study.

Liquid flow results of the same set of filters are found in Figure 4. Again, it can be seen that although the pore geometries are nearly the same for the foam and PLF, PLF flow rates are lower and more consistent. Standard deviations among the 30 ppi foam filters are on the order of 25%, while PLF's have a standard deviation of less than 1%.

To show the utility of the data mapped in Fig. 2, the flow rate of a 30 ppi foam filter was arbitrarily chosen to be matched with a designed PLF. The data in Fig. 2 was used to predict that a PLF

with 13 ppi should have flow properties similar to a 30 ppi foam of similar dimensions. One such 13 ppi filter was robocast. The robocast filter was created in less than five minutes, dried and fired in 24 hours. The resulting flow rate is recorded in Figure 4. In just one attempt the 13 ppi PLF does in fact lie within the standard deviation of the 30 ppi foam. .

It has yet to be determined if the change in pore size will have a large effect on filtration efficiency. Ceramic filters are used in molten metal filtration for two reasons. First, the high temperatures ($>1000^{\circ}\text{C}$) rule out most materials. Second, the filters are attempting to filter out oxides. Since the molten metal being filtered is non-wetting to ceramic oxides, including the filter, small oxide particles in the melt are forced onto the ceramic filter, adding a physical adsorption factor to the mechanical entrapment aspect of filtration. Therefore, even though flow rates are matched by enlarging pore size, it is not necessarily detrimental to filtration.

The additional aspect that a SFF method based on a rapid prototyping machine may be used in conventional manufacturing is attractive. As mentioned before, the supplemental PLF may be fabricated in ~ 5 minutes. It is entirely feasible with this system to build multiple parts in parallel by adding additional tips. Therefore, if 20 parts were built in parallel, 240 parts per hour could be fabricated and fired by the next day, making the step to rapid manufacturing.

Summary:

Periodic lattice filters with good interlayer strength and having a face-centered-cubic structure were robocast. An array of internal pore geometries ranging from 47 to 12.5 ppi were created, and permeability constants were determined for these pore sizes with filter thickness ranging from 4 to 12 layers. Surface areas of these PLF's were calculated and are comparable to extruded honeycomb structures ($>100 \text{ in}^2/\text{in}^3$). Pressure drops of PLF's were higher than foam structures, most likely due to the higher bulk densities and more tortuous pathways in PLF's. In one attempt, a 13 ppi PLF was designed to match the liquid flow rate of a 30 ppi foam. This example of tailored fabrication was completed by using a data map of known pore sizes and sample thickness, and calculating the filter geometry required for a specific flow rate. Part-to-part standard deviations of PLF's are on the order of 1% while foam filters are closer to 25%. Once filtration efficiency has been determined, the usefulness of PLF's in molten metal filtration will be known. However, it is clear that two shortcomings of foam filters have been addressed; the PLF's are much stronger and have more predictable flow characteristics.

Tables and Figures:

Table 1: Correlation of Fired Rod Diameter to PPI and Surface Area for PLF's.

Tip (μm)	Rod Diameter (μm)	Pores per Linear Inch	Surface Area (in^2/in^3)
410	349	47	134
510	434	25	99
840	714	17.5	60
1190	1012	12.5	42

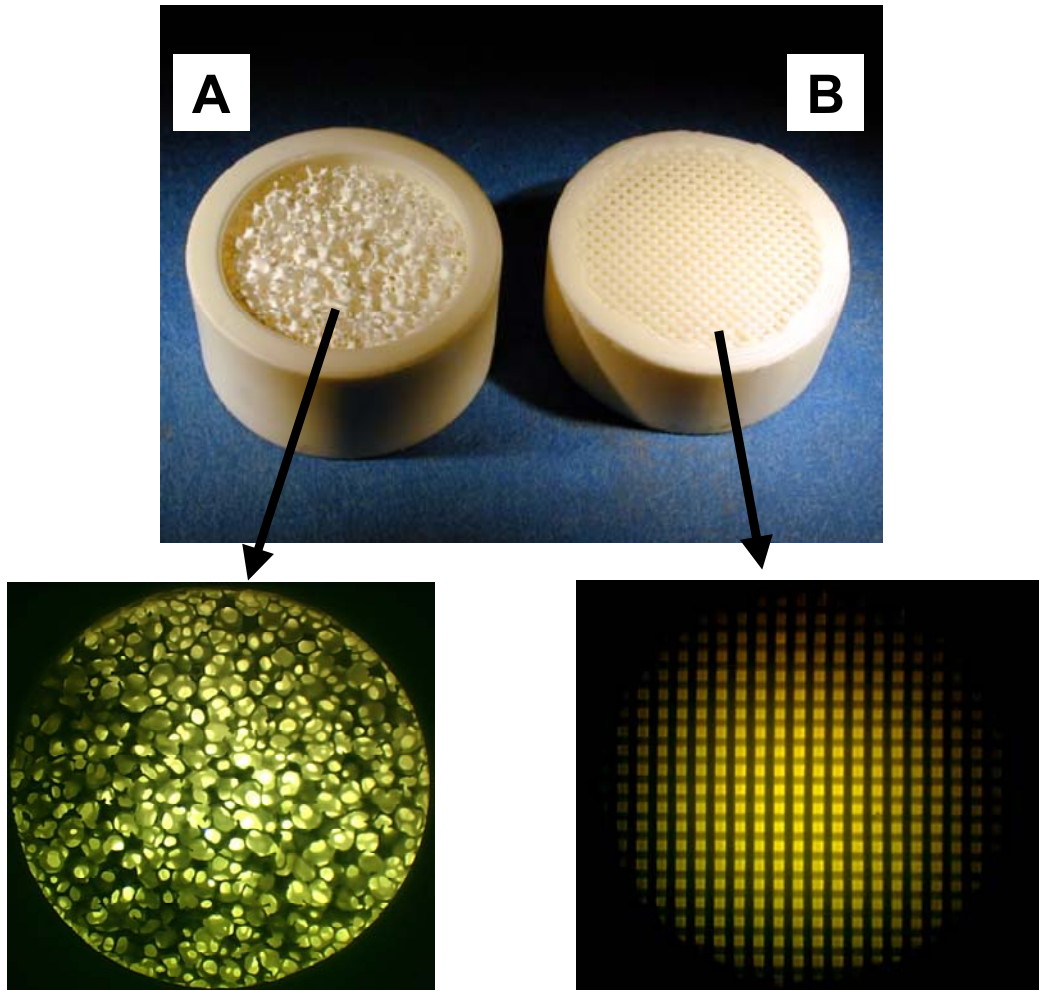


Figure 1: a) 30 ppi ceramic foam filter (courtesy of Selee Corp. SC). b) 30 ppi Robocast PLF. Back-lit images of each show random nature of a) and periodic nature of b).

PREMEABILITY CONSTANT for PLF's

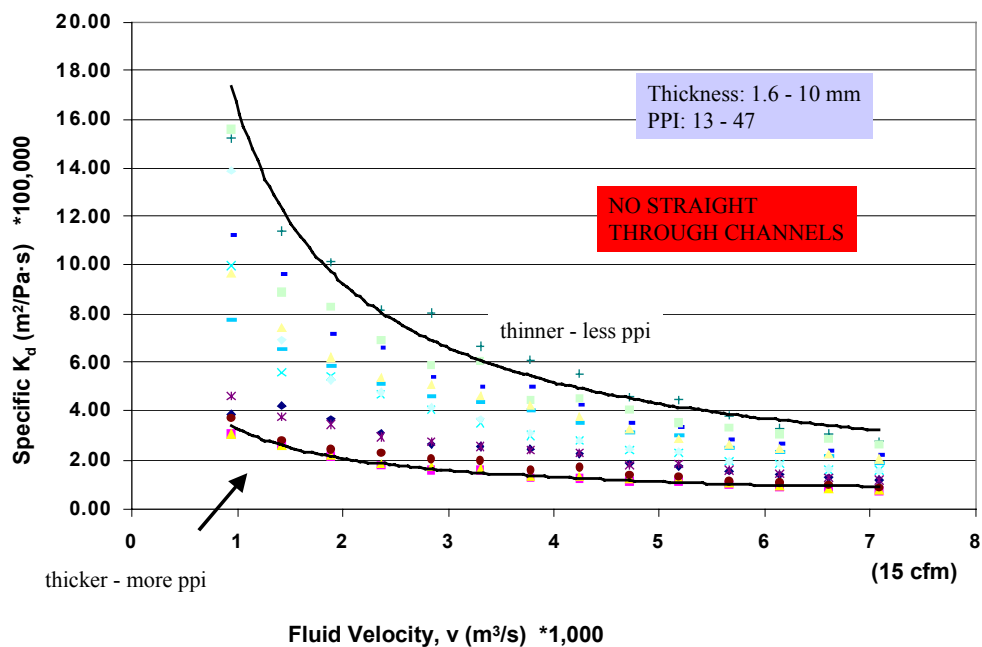


Figure 2: Permeability constants of an array of PLF's. the permeability 'constant' varies with flow rate most likely due to change in flow from turbulent to laminar through the filter.

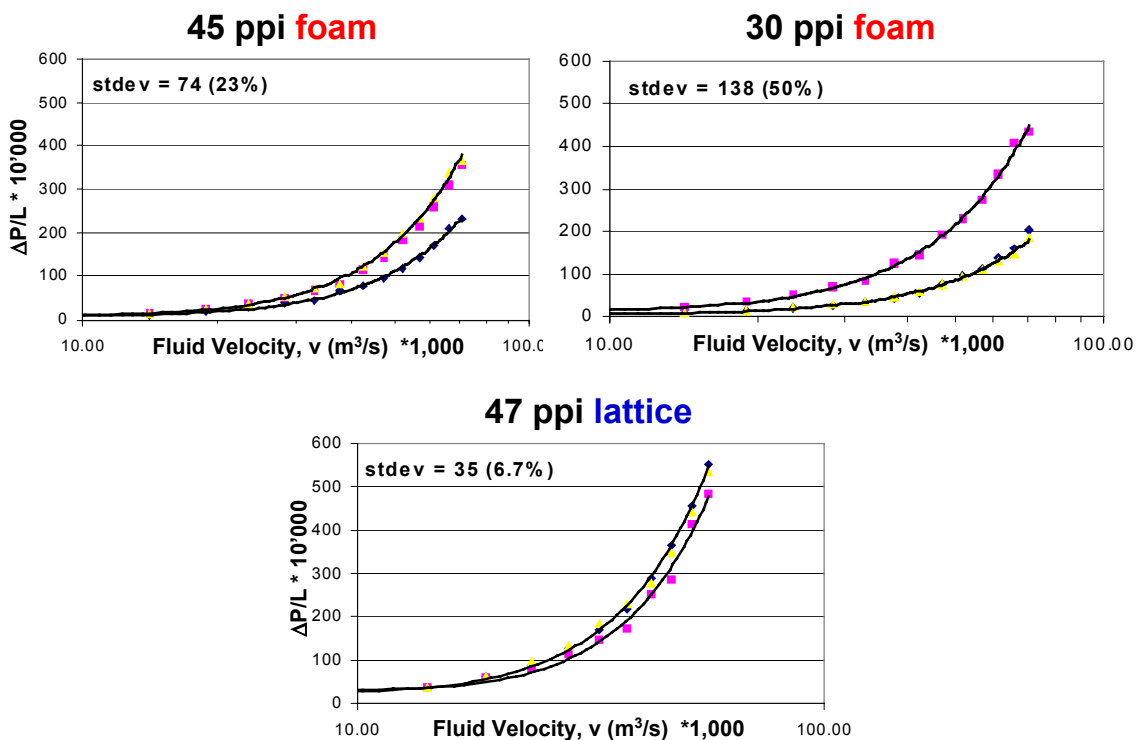


Figure 3: Pressure drop measurements of selected foam and PLF's with high standard deviations being prevalent in foam filters.

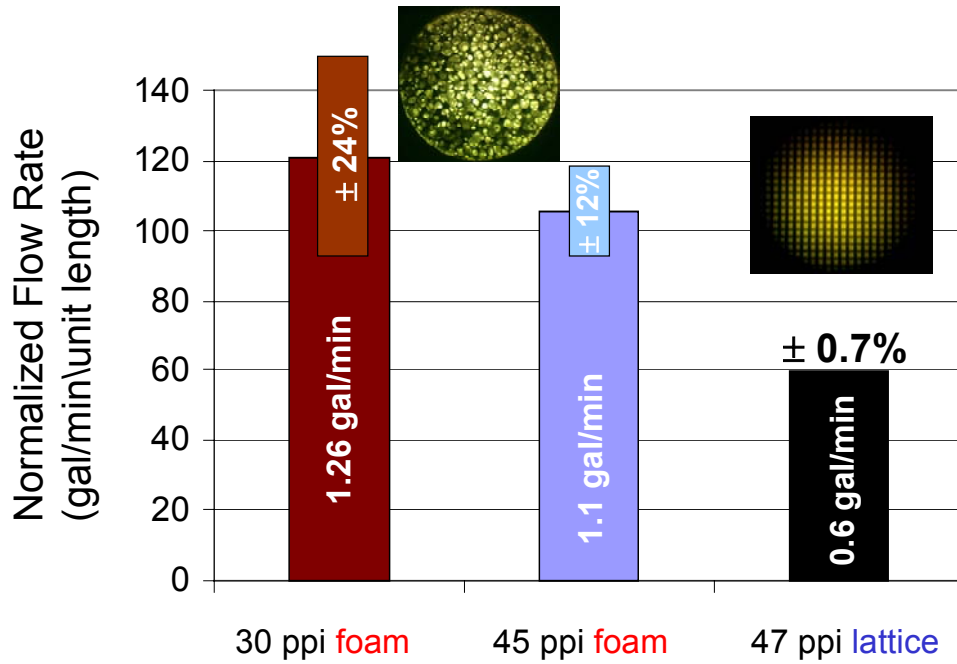


Figure 4: Flow rate measurements of selected foams. The matching PLF has a lower, more predictable flow rate.

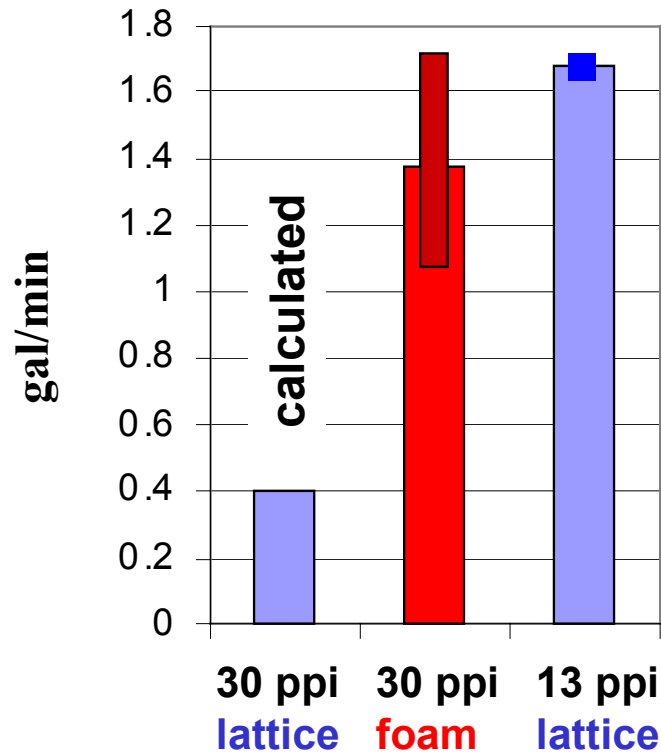


Figure 5: Calculations based on flow rate vs. PLF pore size were employed to match flow rates (in a single attempt) of a PLF to a 30 ppi foam.